

CHAPTER 6 CHARACTERISTICS OF MULTIPLE TLD'S

6.1 MULTIPLE TLD'S AND ITS SIMULATION MODEL

In previous chapters, the frequency response of structure with single TLD was discussed. It has been found that the effectiveness of single TLD is affected significantly by the damping of liquid sloshing. Usually, plain water is used as the liquid in TLD, which possesses relatively low damping. A low damping TLD may not satisfactorily suppress the structural vibrations, so the means to increase damping of liquid sloshing in TLD to the optimal level were studied in Section 5.3. However, it is difficult to maintain the damping of liquid sloshing as the optimal value at any amplitudes of excitation since the damping of liquid sloshing is nonlinear. Moreover, it is difficult to quantitatively evaluate the additional damping, for instance, the damping due to floating surface materials.

Single TLD effectiveness is also sensitive to the tuning condition, i.e., the natural frequency of TLD has to be tuned to that of the structure. The mis-tuning may happen when the structural natural frequency used for design is different from that of the actual structure. Even though tuning is made, this may not hold when wave amplitude of sloshing in TLD is large, resulting in the shift of the natural frequency of TLD due to its nonlinearities. The effectiveness of TLD may become poor under such cases.

Recently, multiple TMD's (MTMD), which consists of a number of small TMD's whose natural frequencies are distributed over a certain range around the natural frequency of the structure (Fig. 6.1). This was proposed by Igusa [1991]. The effectiveness and the sensitivity of MTMD were investigated analytically by Yamaguchi and Harnpornchai [1991] in details. These studies reported that the MTMD are very effectiveness even when the damping of each individual TMD in MTMD is lower than the optimal value of single TMD; a MTMD is more effective than a single TMD when mis-tuning, indicating that the sensitivity of MTMD to the tuning condition is weakened.

With the same concept, the characteristics of multiple TLD's (MTLD) are studied in this chapter on the basis of the simulation of MTLD-structure interaction. In practice, single TLD consists of a number of tanks with same size and same liquid depth to meet required liquid mass in total. By changing the

liquid depth in each TLD tank, it is very easy to have a number of TLD's, i.e., MTLD, whose natural frequencies are distributed over certain range (Fig. 6.2).

Figure 6.1 Igusa's multiple TMD (MTMD).

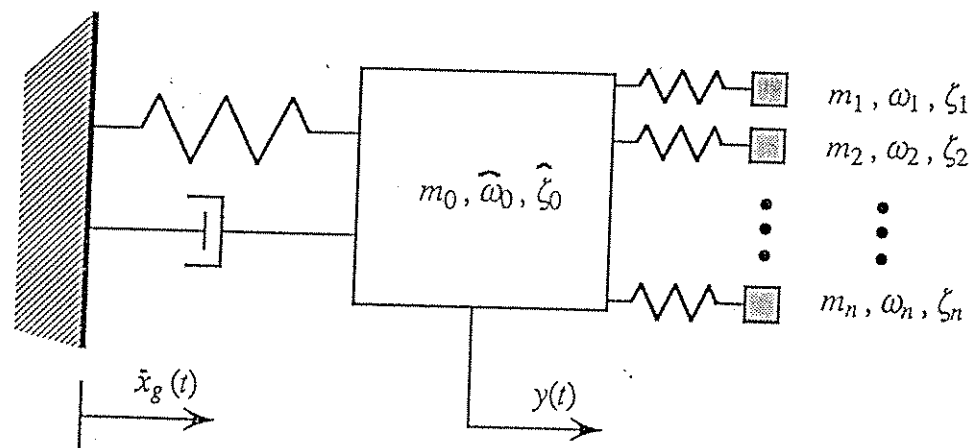
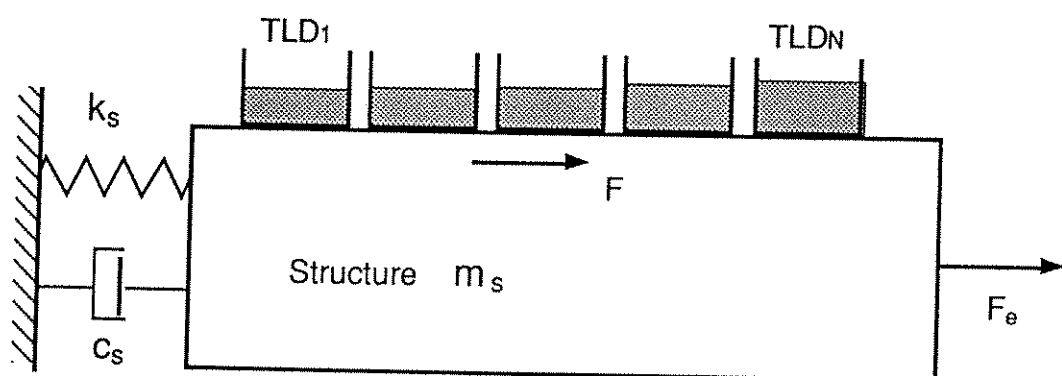
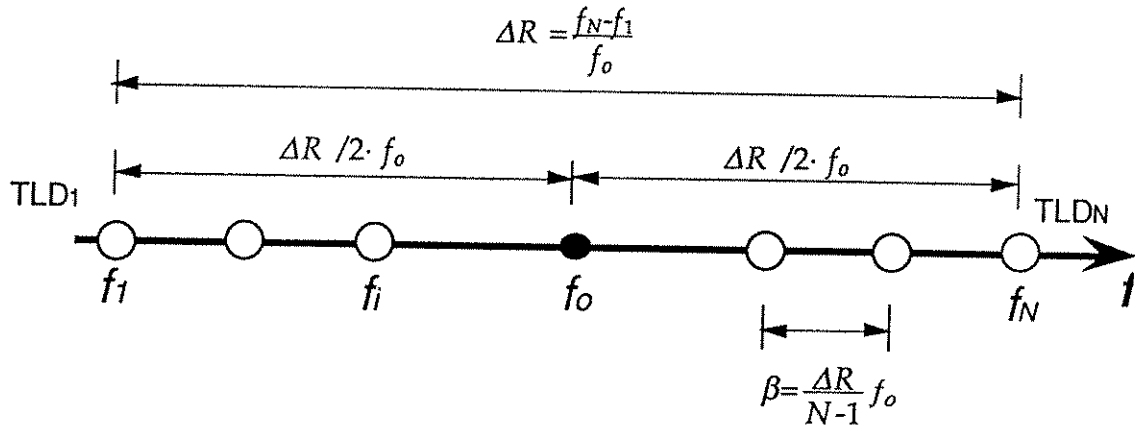


Figure 6.2 The multiple TLD (MTLD).



By using the TLD model proposed, the MTLD-structure interaction were simulated. At each time step, the base shear force of each TLD under the excitation of structure was calculated and the total force due to the TLD's was obtained. Then the structural response at the next time step under this total force was computed. The computation was continued until the structural response became a steady state.

Figure 6.3 Frequency distribution of MTLD.



In Igusa's paper [1991], he assumed that the MTMD have equal frequency spacing, equal damping and equal mass. In this study, the MTLD with equal frequency spacing was used. However, since the TLD tanks with same size were used usually in practice, each individual TLD in MTLD had slightly different damping or mass owing to the variation of the liquid depth. The simulations were carried out with the aim of studying the effects of TLD on its characteristics by several parameters, such as: TLD number, N and the frequency distribution range, ΔR (Section 6.2), mis-tuning factor, $\Delta\gamma$ (Section 6.3), and the center liquid depth ratio ε_o (Section 6.4). In the simulation, a number of tanks with same size ($2a=59.0\text{cm}$, $b=33.5\text{cm}$) were used. The liquid depth for each individual TLD was varied to make MTLD have equal frequency spacing, β , so the mass and the

damping for each individual TLD were slightly different. The mass ratio μ , i.e., the ratio of the total mass of MTLD to that of the structure, is 1%. As shown in Fig.6.3, the frequency distributions of MTLD can be described by two quantities: the center frequency of MTLD, f_o and the frequency distribution range, ΔR of MTLD. f_o and ΔR are expressed as

$$f_o = \frac{f_N + f_1}{2} \quad (6.1)$$

$$\Delta R = \frac{f_N - f_1}{f_o} \quad (6.2)$$

where f_1 and f_N are the lowest and the highest natural frequency of individual TLD, respectively. For studying the sensitivity of MTLD at the mis-tuning condition, the mis-tuning factor, $\Delta\gamma$ is defined as

$$\Delta\gamma = \frac{f_s - f_o}{f_o} \quad (6.3)$$

where, f_s is the natural frequency of structure. The SDOF structure with a structural damping ratio of $\xi_s=0.32\%$ was excited sinusoidally by a external force with constant amplitude. For simplicity, a small external force was used in the studies mentioned above (Sections 6.2-6.4). This force made that the structural amplitude without damper is 0.1cm at the resonance. So the liquid sloshing in TLD's was considered to be linear under such a small base amplitude.

In addition, the effects of the nonlinearities of MTLD due to the large amplitude excitation were also studied in Section 6.5.

6.2 EFFECTS OF NUMBER AND FREQUENCY DISTRIBUTION RANGE OF MTLD

The simulations were done with various number of TLD's (Table 6.1) and the results are shown in Fig. 6.4. The central frequency f_o is 0.458 Hz, corresponding to a liquid depth $h_o=3.0$ cm. The frequency distribution range ΔR is 0.2, i.e., the MTLD's are distributed in the frequency range of $0.90 \leq f_i/f_o \leq 1.10$. The structural frequency f_s is 0.458Hz and the resonance amplitude A without damper is 0.1cm. So the wave amplitude is small and the wave motion is regarded to be linear. For comparison, the structural response with single TLD (STLD) is also plotted in Fig. 6.4. Both MTLD and STLD have the mass ratio $\mu=1\%$.

Table 6.1 Simulation cases for effects of number of TLD's.

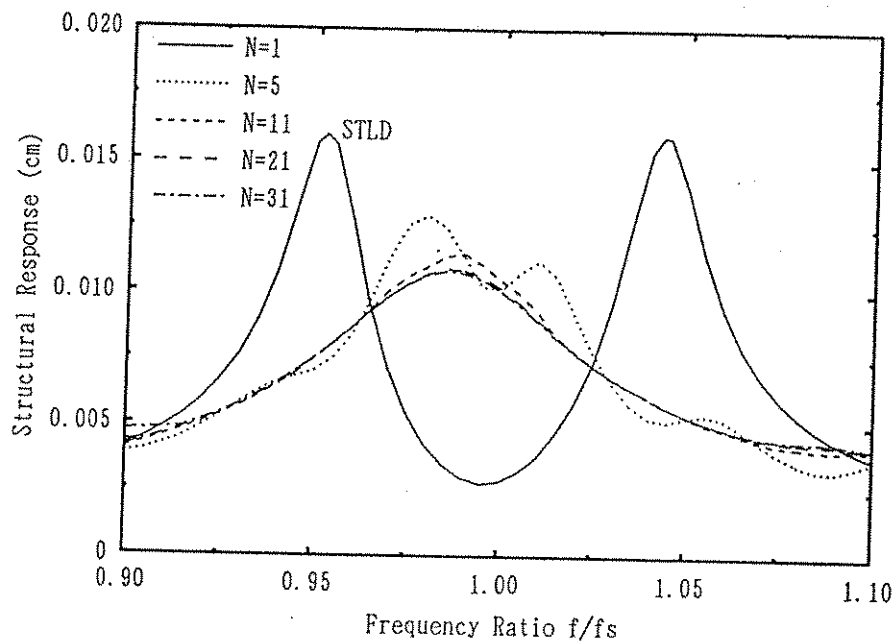
| Case name | N | ΔR | $f_o(\text{Hz})$ | $f_s(\text{Hz})$ | $A(\text{cm})$ |
|-----------|-----|------------|------------------|------------------|----------------|
| A01R0N01 | 1 | - | 0.458 | 0.458 | 0.1 |
| A01R2N05 | 5 | 0.2 | 0.458 | 0.458 | 0.1 |
| A01R2N11 | 11 | 0.2 | 0.458 | 0.458 | 0.1 |
| A01R2N21 | 21 | 0.2 | 0.458 | 0.458 | 0.1 |
| A01R2N31 | 31 | 0.2 | 0.458 | 0.458 | 0.1 |

Table 6.2 Simulation cases for effects of frequency ratio range of TLD's.

| Case name | N | ΔR | $f_o(\text{Hz})$ | $f_s(\text{Hz})$ | $A(\text{cm})$ |
|-----------|-----|------------|------------------|------------------|----------------|
| A01R0N01 | 1 | - | 0.458 | 0.458 | 0.1 |
| A01R1N05 | 5 | 0.1 | 0.458 | 0.458 | 0.1 |
| A01R2N05 | 5 | 0.2 | 0.458 | 0.458 | 0.1 |
| A01R4N05 | 5 | 0.4 | 0.458 | 0.458 | 0.1 |
| A01R1N21 | 21 | 0.1 | 0.458 | 0.458 | 0.1 |
| A01R2N21 | 21 | 0.2 | 0.458 | 0.458 | 0.1 |
| A01R4N21 | 21 | 0.4 | 0.458 | 0.458 | 0.1 |

From Eq.(5.11), we know that the damping of STLD used herein is about 2%. This value is lower than the optimal one, ($\approx 6\%$ in the case of the mass ratio $\mu=1\%$). The structural response with the low damping STLD has two peaks around the frequency ratio f/f_s , 0.95 and 1.05. When using MTLD, the maximum response of the structure becomes lower and the curve shape varies from 2 peaks type (STLD) to 1 peak type (MTLD). It is found that MTLD is more effective than STLD even they have same mass ratio.

Figure 6.4 Effects of number of TLD's.



When using 5 TLD's, the response curve has several local peaks. The curve becomes smooth when increasing the TLD number N to 11, also, the maximum response is reduced slightly. Then increasing N to 21 or even 31, the response curve does not change so much. The effectiveness of MTLD is not sensitive to the TLD numbers N . A MTLD with $N=5-11$ have good effectiveness. So the most of simulation cases in later sections used $N=5$.

Figure 6.5 Effects of frequency distribution range of MTLD.

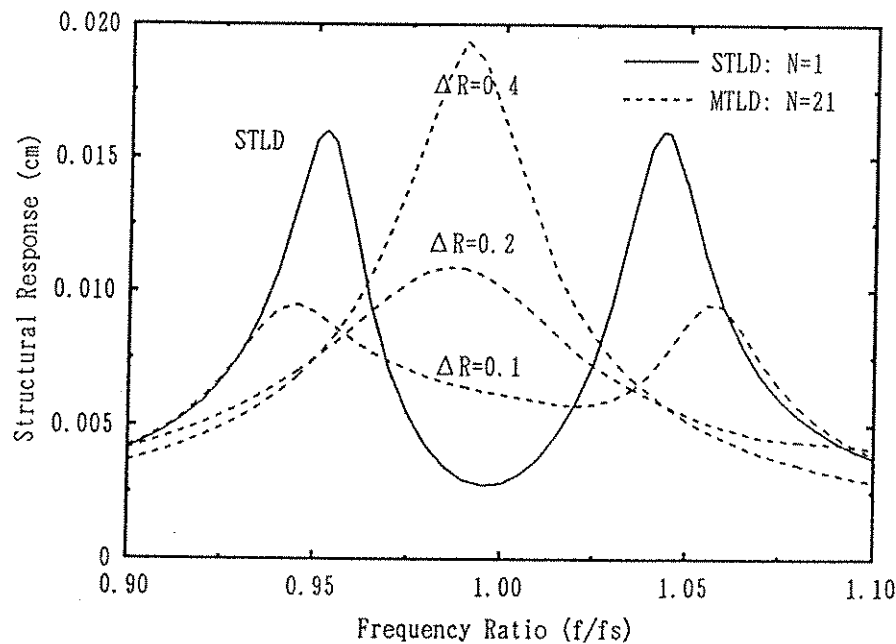


Figure 6.5 shows the effects of the frequency distribution range, ΔR of MTLD. The simulation cases are as described in table 6.2, The structural responses with 3 types of MTLD, i.e., $\Delta R=0.1$ ($0.95 < f_i/f_o < 1.05$), $\Delta R=0.2$ ($0.90 < f_i/f_o < 1.05$); and $\Delta R=0.4$ ($0.80 < f_i/f_o < 1.20$) are computed. The number of TLD, N is 21. The results show that MTLD with $\Delta R=0.1$ mostly reduced the maximum structural response as compared with that attached STLD. When MTLD with $\Delta R=0.4$ used, the maximum response located near the $f/f_s=1.00$ becomes larger even than that with STLD. The frequency distribution of MTLD has an optimal range to make the structural response minimum. Compared with the results shown in Fig. 6.4, it is found that the effectiveness of MTLD is more sensitive to the frequency distribution range ΔR than to the number N .

6.3 EFFECTIVENESS OF MIS-TUNING MTLD

In this section, the effectiveness of MTLD mis-tuning to a structure is discussed. TLD has to be designed to tune to the frequency of a target structure. However, the mis-tuning may happened sometimes. The mis-tuning factor, $\Delta\gamma$ is defined by Eq. (6.3). The condition used in the simulation are the same as that in Section 6.2 except the structural frequency f_s (Table 3.5). Fig. 6.6a shows the structural responses with tuning STLD and mis-tuning STLD, i.e., $f_s=f_o$, $f_s=0.95f_o$ ($\Delta\gamma=-5.0\%$) and $f_s=1.05f_o$ ($\Delta\gamma=5.0\%$). It can be seen that the maximum structural response become larger due to the mis-tuning compared with the tuning case.

Table 6.3 Simulation cases for effects of mis-tuning of MTLD.

| Case name | N | ΔR | $f_o(\text{Hz})$ | $f_s(\text{Hz})$ | $\Delta\gamma$ | $A(\text{cm})$ |
|-------------|-----|------------|------------------|------------------|----------------|----------------|
| A01R0N01 | 1 | - | 0.458 | 0.458 | tuning | 0.1 |
| A01R0N01.S3 | 1 | - | 0.458 | 0.435 | -5.0% | 0.1 |
| A01R0N01.S4 | 1 | - | 0.458 | 0.481 | 5.0% | 0.1 |
| A01R1N05 | 5 | 0.1 | 0.458 | 0.458 | tuning | 0.1 |
| A01R1N05.S3 | 5 | 0.1 | 0.458 | 0.435 | -5.0% | 0.1 |
| A01R1N05.S4 | 5 | 0.1 | 0.458 | 0.481 | 5.0% | 0.1 |
| A01R2N05 | 5 | 0.2 | 0.458 | 0.458 | tuning | 0.1 |
| A01R2N05.S3 | 5 | 0.2 | 0.458 | 0.435 | -5.0% | 0.1 |
| A01R2N05.S4 | 5 | 0.2 | 0.458 | 0.481 | 5.0% | 0.1 |
| A01R4N05 | 5 | 0.4 | 0.458 | 0.458 | tuning | 0.1 |
| A01R4N05.S3 | 5 | 0.4 | 0.458 | 0.435 | -5.0% | 0.1 |
| A01R4N05.S4 | 5 | 0.4 | 0.458 | 0.481 | 5.0% | 0.1 |

Mis-tuning MTLD ($N=5$) with various frequency distribution range, $\Delta R=0.1$, 0.2 , 0.4 were simulated and the results are plotted in Figs. 6.6b, c, and d, respectively. It is found that the MTLD with $\Delta R=0.2$ is insensitive to the tuning condition, namely, the maximum structural response dose not vary too much even the MTLD mis-tune to the structure (Fig. 6.6c). The MTLD with $\Delta R=0.1$ although mostly reduced the structural response when it tuns, the effectiveness becomes poor under mis-tuning condition (Fig. 6.6b). The MTLD with $\Delta R=0.1$, is also not effective in the case of mis-tuning (Fig. 6.6d).

Figure 6.6a Effectiveness of TLD under mis-tuning condition (STLD).

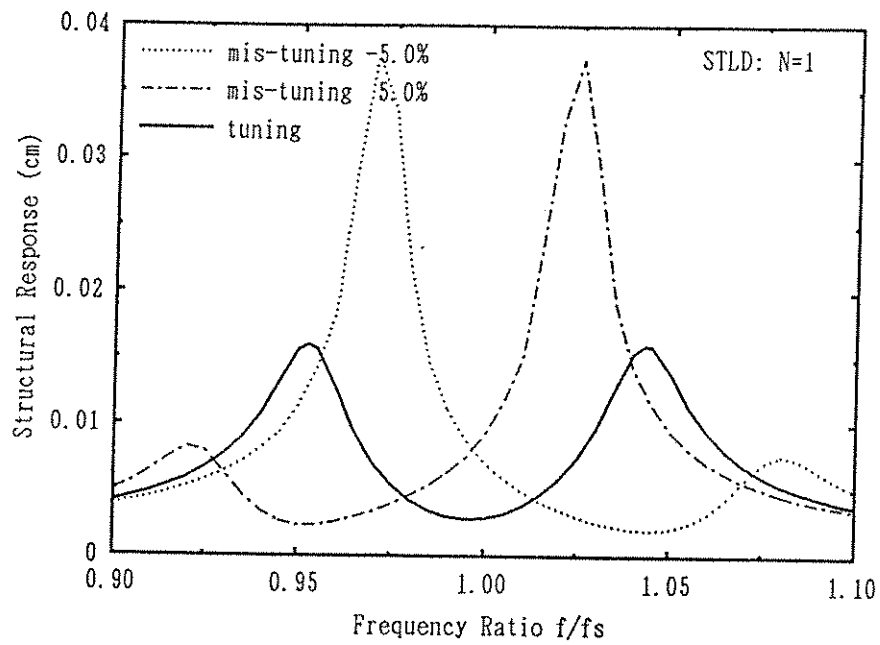


Figure 6.6b Effectiveness of TLD under mis-tuning condition (MTLD, $\Delta R=0.1$).

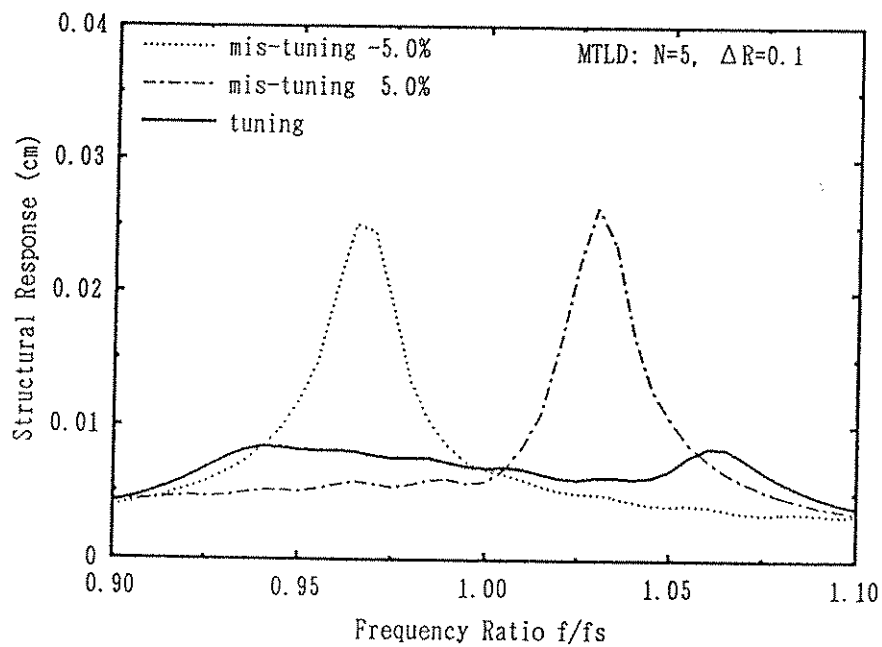


Figure 6.6c Effectiveness of TLD under mis-tuning condition (MTLD, $\Delta R=0.2$).

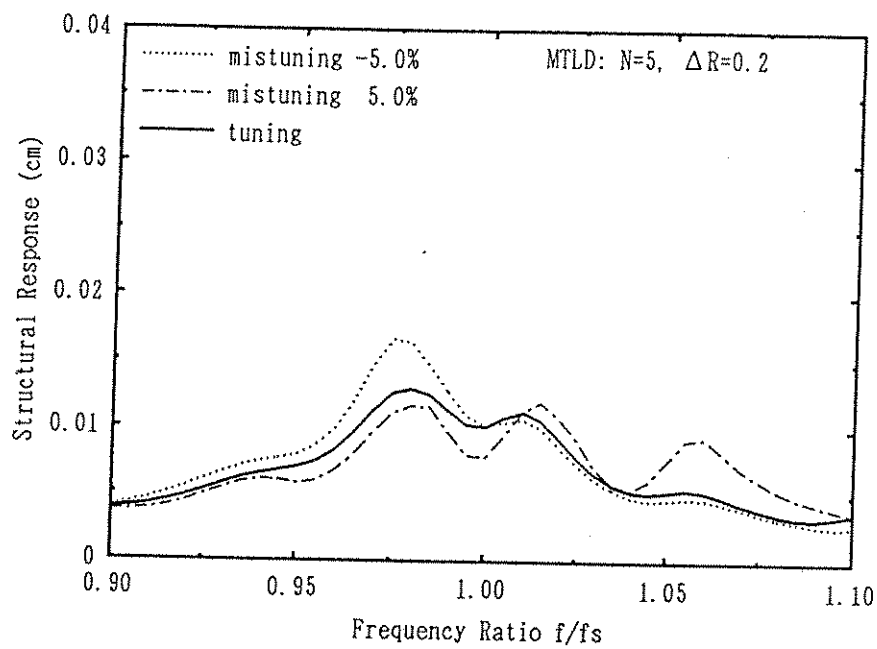
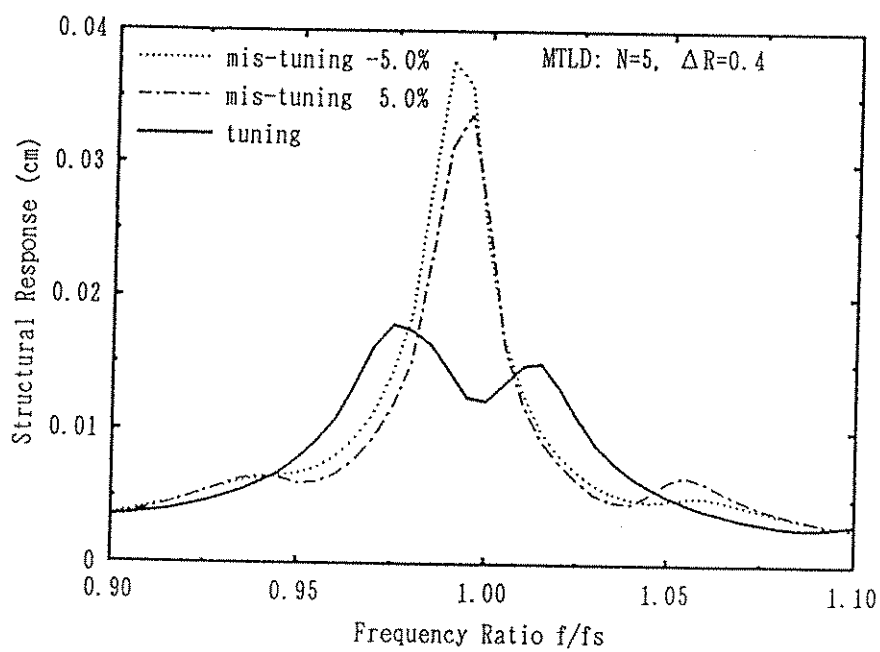


Figure 6.6d Effectiveness of TLD under mis-tuning condition (MTLD, $\Delta R=0.4$).



6.4 EFFECTS OF CENTER LIQUID DEPTH RATIO

TLD with different liquid depth ratio has different damping. The effects of liquid depth (or damping of liquid sloshing) are discussed in this section.

Table 6.4 Simulation cases for effects of liquid depth ratio.

| Case name | N | ΔR | $f_o(\text{Hz})$ | $f_s(\text{Hz})$ | ε_o | $A(\text{cm})$ |
|-------------|-----|------------|------------------|------------------|-----------------|----------------|
| A01R0N01 | 1 | - | 0.458 | 0.458 | 0.1 | 0.1 |
| A01R1N05 | 5 | 0.1 | 0.458 | 0.458 | 0.1 | 0.1 |
| A01R0N01.H6 | 1 | - | 0.639 | 0.639 | 0.2 | 0.1 |
| A01R1N05.H6 | 5 | 0.1 | 0.639 | 0.639 | 0.2 | 0.1 |

The MTLD with $\varepsilon_o=0.1, 0.2$ are shown in Figs. 6.7a and 6.7b. Note that the same size TLD tanks were used for these two cases, so the center frequencies of MTLD are 0.458 Hz and 0.639 Hz, respectively. The structural frequencies tune to the MTLD (Table 6.4). From Eq. (5.11), it can be known that the liquid damping is inversely proportional to liquid depth ratio, so the damping of center TLD in MTLD (i.e., $f_i=f_o$) with $\varepsilon_o=0.1$ is about two times of that in MTMD with $\varepsilon_o=0.2$.

Figure 6.7a Effects of central liquid depth ratio ($\varepsilon_o=0.1$).

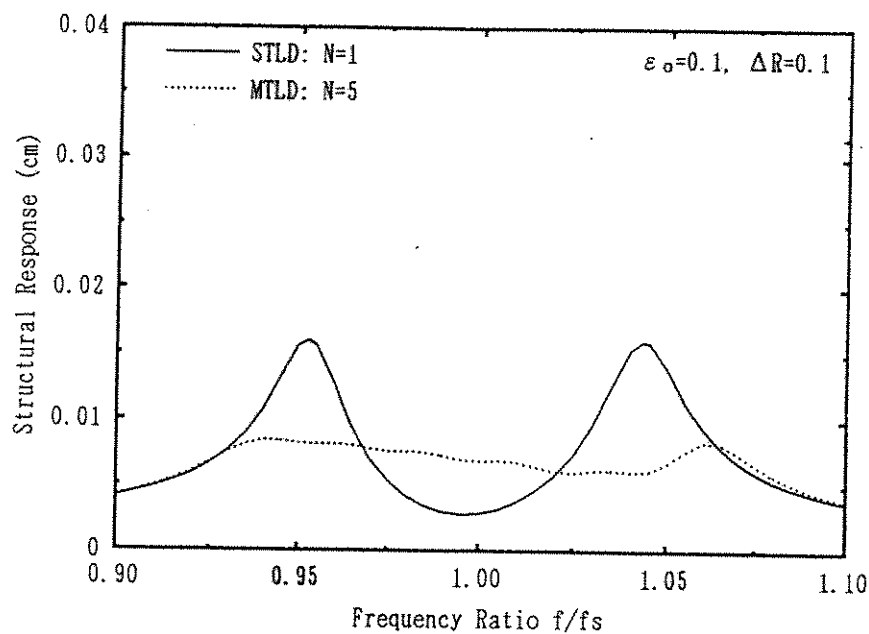
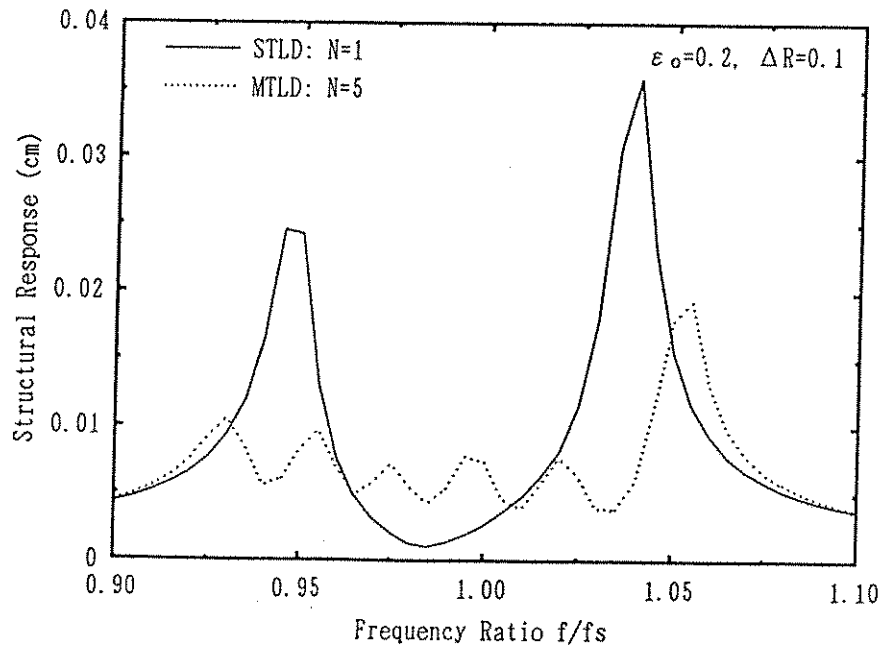


Figure 6.7b Effects of Center Liquid Depth Ratio ($\epsilon_0=0.2$).



From Fig. 6.7, it can be found that both STLD and MTLD with small depth ratio ($\epsilon_0=0.1$) have better effectiveness (Fig. 6.7a) than that with large one ($\epsilon_0=0.2$) (Fig. 6.7b). When using MTLD, the maximum structural responses are reduced to half of that using STLD. The response with MTLD with $\epsilon_0=0.2$ (Fig. 6.7b) have several local peaks since the liquid sloshing has small damping. This is similar to the case using small damping MTMD as discussed by Yamaguchi et al. [1991]. By increasing the damping of MTLD with $\epsilon_0=0.2$ to certain value, the effectiveness of the MTLD can be improved.

6.5 EFFECTS OF EXCITATION AMPLITUDE

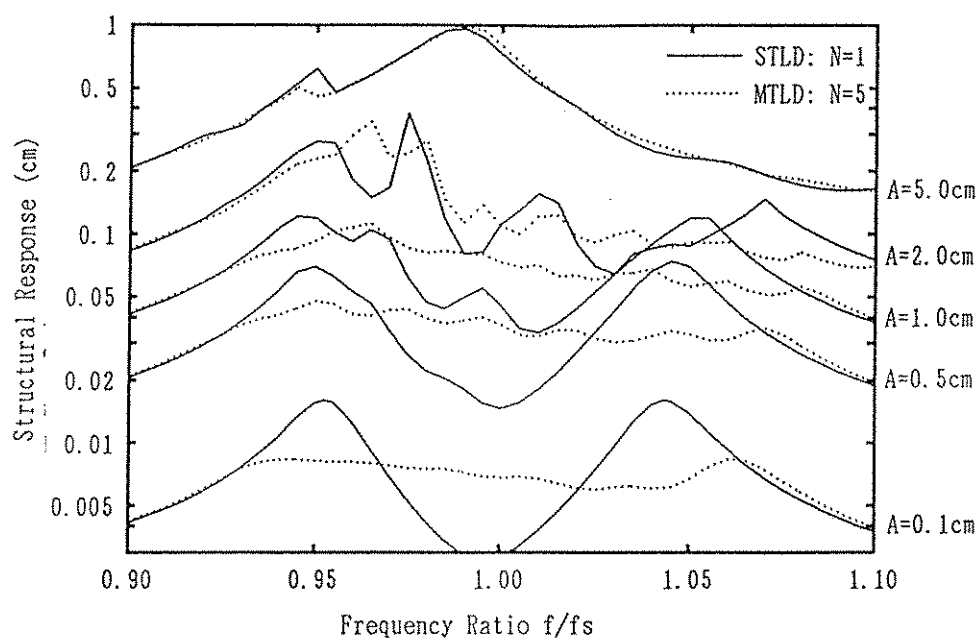
As discussed in Section 5.1, the liquid sloshing becomes nonlinear under large amplitude base excitation. The nonlinearities of liquid sloshing may affect the performances of MTLD. The structural responses with various values of A which is the resonant amplitude of structure response without damper were simulated (Table 6.5) in order to study the effects of the nonlinearities.

Table 6.5 Simulation cases for effects of amplitude of structure.

| Case name | N | ΔR | $f_o(Hz)$ | $f_s(Hz)$ | $A(cm)$ |
|-----------|-----|------------|-----------|-----------|---------|
| A01R0N01 | 1 | - | 0.458 | 0.458 | 0.1 |
| A01R1N05 | 5 | 0.1 | 0.458 | 0.458 | 0.1 |
| A05R0N01 | 1 | - | 0.458 | 0.458 | 0.5 |
| A05R1N05 | 5 | 0.1 | 0.458 | 0.458 | 0.5 |
| A10R0N01 | 1 | - | 0.458 | 0.458 | 1.0 |
| A10R1N05 | 5 | 0.1 | 0.458 | 0.458 | 1.0 |
| A20R0N01 | 1 | - | 0.458 | 0.458 | 2.0 |
| A20R1N05 | 5 | 0.1 | 0.458 | 0.458 | 2.0 |
| A50R0N01 | 1 | - | 0.458 | 0.458 | 5.0 |
| A50R1N05 | 5 | 0.1 | 0.458 | 0.458 | 5.0 |

For the cases with $A=0.1cm$ and $0.5cm$, the liquid sloshing appears linear, so the maximum response of the structure is significantly reduced by using MTLD. The effects of the nonlinearities of MTLD can be observed from the cases where $A \geq 1.0cm$. There are several local peaks on the response curves of the cases $A=1.0cm$ and $A=2.0cm$, indicating the effects of the higher harmonics of liquid sloshing. The maximum structural responses for these two cases do not change so much even using MTLD. For the case $A=5.0cm$, it is known from the simulation that the breaking waves occurred. The structural response is almost the same either using STLD or using MTLD.

Figure 6.8 Effects of excitation amplitude.



6.6 SUMMARY

The effectiveness of TLD can be improved by using MTLD even with small damping if a suitable frequency distribution range are used. The effectiveness of MTLD is sensitive to the frequency range over where the MTLD are distributed, but is not so significantly affected by the number of MTLD.

MTLD with a suitable frequency distribution range is effective for suppressing the vibrations of a mis-tuned structure .

The improvement by using MTLD over STLD is not significant when the liquid sloshing in TLD is strongly nonlinear. MTLD has almost the same effectiveness as STLD when the breaking waves occur.

TLD in practice consists of a number of tanks with same size filled by water. The damping of water sloshing is small and this gives a negative effect to the performance of TLD. It is easy to design a MTLD by using a number of tanks filled by slightly different liquid depth and no need to try to increase the damping of water sloshing to an optimal value as did for STLD. The MTLD is very attractive for application.

CHAPTER 7 CONCLUSIONS

A two-dimensional nonlinear model for liquid sloshing in a rectangular TLD under horizontal motion was proposed previously by the author based on the shallow water wave theory. The model is improved in this study with emphasis on the damping of liquid sloshing. Its validity is assessed by the shaking table experiment. It is shown that the model can describe liquid sloshing in TLD, moreover the response of structure with attached TLD with satisfactory accuracy.

The proposed model is extended to be able to deal with the liquid sloshing in a TLD subjected to pitching motion. The simulations by the model agree well with the experimental results, indicating that the model is valid for predicting liquid sloshing under pitching motion. The simulations by the model reveal that the TLD attached to a structure under pitching motion is very effective even with a small ratio of moment of inertia.

Breaking wave is a significant phenomenon of liquid sloshing in TLD, and it gives high damping to liquid sloshing. The model for liquid sloshing under horizontal motion is modified by introducing two coefficients C_{da} and C_{fr} in the basic equations, which stand for the effects of breaking waves on the damping and the natural frequency of liquid sloshing, respectively. C_{da} and C_{fr} are determined by the shaking table experiments. This modified model is experimentally assessed. It is found that it can predict the structural responses with attached TLD even when breaking waves present.

The SOLA-VOF code is employed to simulate liquid sloshing. It is however found that the code is not valid for an engineering application to predict the liquid sloshing with breaking waves. Much effort must be devoted for the improvement of the SOLA-VOF method.

Both the experiments and the theoretical simulations show that the liquid sloshing in TLD is strongly nonlinear and reveals hardening-spring property when liquid is shallow. Higher harmonics of liquid sloshing which have natural frequencies of approximately odd number times of the fundamental one,

contribute some effects near the primary resonance and make the liquid sloshing properties more complicated.

The basic parameters affecting TLD effectiveness are discussed on the basis of theoretical studies. These parameters are affected by several physical quantities such as TLD tank size, liquid depth, and liquid viscosity. The relations between them are discussed. These discussions are also expected to be helpful for TLD design.

The mechanism of TLD is explained based on the understanding to that of Tuned Mass Damper (TMD), a well-known mechanical damper. Similar to TMD, TLD is installed to a structure to suppress vibrations of structure by shutting out the input energy to the structure and by dissipate the vibrational energy. The damping of liquid sloshing is a significant parameter affecting the effectiveness of TLD. It is found that the effectiveness of TLD is comparable to that of TMD if the damping of liquid sloshing is controlled to a suitable level.

Usually plain water is used as the liquid in TLD. The damping of liquid sloshing in such case is much lower than the optimal value since as the viscosity of water is low. The experimental studies show that the damping of liquid sloshing can be increased by using shallow liquid, using high-viscosity liquid, and adding floating materials on free surface of liquid. It is found that the effectiveness of TLD can be improved by increasing the damping of liquid sloshing.

The effectiveness of multiple TLD is studied by the simulations. It is found that the multiple TLD is more effective than a single TLD even with low damping; and the MTLD is insensitive to the tuning condition. The multiple TLD design is a very attractive concept for application.

Active TLD should be studied in the future.

REFERENCES

- Abramson, H. N., "The Dynamic Behavior of Liquids in Moving Containers." NASA SP-106, 1966.
- Bauer, H.F., "Nonlinear Propellant Sloshing in a Rectangular Container of Infinite Length." Development in Theoretical and Applied Mechanics. Vol.3, 1969, pp725-759.
- Bhuta, P. G., and Koval, L. R., "A Viscous Ring Damper for a Freely Precessing Satellite," Int. J. Mechanical Science, Vol. 8, 1966, pp. 383-395.
- Chaiseri, P., Fujino, Y., Pacheco, B. M. and Sun, L. M., "Interaction of Tuned Liquid Damper (TLD) and Structure - Theory, Experimental Verification and Application -," J. Struc. Eng./Earthq. Eng., Proc. JSCE, Vol. 6, No. 2, 1989, pp. 273-282.
- Chaiseri, p., "Characteristics, Modelling and Application of the Tuned Liquid Damper," Doctoral Thesis, Dept. of Civil Eng., The Univ. of Tokyo, 1990, 204pp.
- Chester, W., "Resonant Oscillation of Water Waves. I. Theory & II. Experiment," Proceedings, Royal Society of London, A306, 1968, pp.5-39.
- Fujii, K., Tamura, Y., Sato, T., and Wakahara, T., "Wind-Induced Vibration of Tower and Practical Applications of Tuned Sloshing Damper," J. of Wind Engineering, Japan Association for Wind Engineering, No. 37, 1988, pp. 537-546.
- Fujino, Y., "Control of Wind-Induced Vibrations in Civil Engineering Structure," J. of Wind Eng., Japan Association for Wind Eng., No.44, 1990, pp.53-69. (In Japan).
- Fujino, Y., Pacheco, B. M., Chaiseri, P., and Sun, L. M., "Parametric Studies on Tuned Liquid Damper (TLD) Using Circular Containers By Free-oscillation Experiment," J. Struc. Eng./Earthq. Eng., JSCE., Vol. 5, No. 1, 1988, pp. 381-391.
- Fujino, Y., Pacheco, B., M., Chaiseri, P., Sun, L. M., and Koga, K, "Understanding of TLD Properties Based on TMD Analogy," JSCE, J. Struc. Eng., Vol.36A, 1990, pp. 577-590. (In Japanese).
- Hayama, S., Aruga, K., and Watanabe, T., "Nonlinear Sloshing in Rectangular Tank." Proceedings, JSME(C), Vol.49, No.437, pp22-30 (In Japanese).
- Horikawa, K., "Coastal Engineering," University of Tokyo Press, 1978, Chapter 2.
- Igusa, T., Xu, K., "Vibration Reduction Characteristics of Distributed Tuned Mass Dampers," Proc., 4th Intl. Conf., Structural Dynamics: Recent Advances, Southampton, UK, 1991, pp.596-605.
- Jonsson, I. G., "Wave Boundary Layer and Friction Factors," Proc. of 10th CCE, ASCE, 1966, pp. 127-148.

- Koga, K., "The Application of Tuned Liquid Damper to Torsional Vibration," Master's Thesis, Dept. of Civil Eng., The Univ. of Tokyo, 1990, 69pp.
- Lamb, H., "Hydrodynamics," Cambridge Univ. Press, 6th Edition, 1932, pp. 619-621.
- Lepelletier, T. G., and Raichlen, F., "Nonlinear Oscillations in Rectangular Tanks," J. of Engineering Mechanics, Vol.114(1), ASCE., 1988, pp. 1-23.
- Lepelletier, T. G., "Tsunamis-Harbor Oscillations Induced by Nonlinear Transient Long Waves," W. M. Keck Lab Report, No.KH-R-41, California Institute of Technology, 1980, 481pp.
- Miles, J. W., "Nonlinear Surface Waves in Closed Basins," J. Fluids Mech., Vol.75, 1976, pp.419-448.
- Miles, J. W., "Surface Wave Damping in Closed Basins," Proc. Royal Society of London, A 297, 1967, pp. 459-475.
- Miyata, H., Kajitani, H., Zhu, M., and Kawano, t., "Numerical Study of Some Wave-Breaking Problems by a Finit-Difference method," J. Kansai Soc. Nav. Archit., Japan, No.207, 1987, pp.11-23.
- Miyata, T., Yamada, H., and Saitoh, Y., "Feasibility Study of the Sloshing Damper System Using Rectangular Containers," JSCE, J. Struc. Eng., Vol.35A, 1989, pp.553-560. (In Japanese).
- Modi, V. J., and Welt, F., "Vibration Control Using Nutation Dampers," Proc. Int. Conf. on Flow Induced Vibrations, England, 1987, pp. 369-376.
- Nakayama, T. and Washizu, K., "The Boundary Element Method Applied to the Analysis of Two-Dimensional Nonlinear Sloshing Problems," International Journal for Numerical Method in Eng., Vol.17, 1981, pp.1631-1646.
- Nayfeh, A. H., and Mook, D. T., "Nonlinear Oscillations," John Wiley & Sons, Inc., 1979, pp.161-257.
- Nichols, B. D., Hirt, C. W., and Hotchkiss, R.S., "SOLA-VOF: A Solution Algorithm for Transient Fluid Flow with Multiple Free Boundaries," Los Alams Scientific Laboratory report LA-8355, 1980.
- Noji, T., Yoshida, H., Tatsumi, E., and Hagiuda, H., "Study on Vibration Control Damper Utilizing Sloshing of Water," J. of Wind Engineering, Japan Association for Wind Engineering, No. 37, 1988, pp. 557-566.
- Nozawa, K., "Damping Control of Liquid Sloshing in a tank," Graduated Thesis, Dept. of Civil Eng., Univ. of Tokyo, 1990, 57pp. (In Japanese).
- Ohyama, T. and Fujii, K., "A Boundary Element Analysis for Tow-Dimentional Nonlinear Sloshing Problems," JSCE, J. Struc. Eng., Vol.35A, 1989, pp. 575-584. (In Japanese).

- Ohyama, T., "Nonlinear Sloshing Motion in a Circular Basin," Proc. JSCE, No.417/II-13, 1990, pp. 255-264. (In Japanese).
- Pacheco, B.M., "Mass and Dashpot Representation of Nonlinear Passive Mechanical Dampers," Proc. 44th JSCE Annul Meeting, Vol.1, 1989, pp.736-737. (In Japanese).
- Sakai, F., Takaeda, S., and Tamaki, T., "Vibration Experiment on Effect of Tuned Liquid Column Damper (TLCD) Using a Similitude Model," JSCE, J. Struc. Eng., Vol. 36A, 1990, pp. 603-613. (In Japanese).
- Sato, T., "Tuned Sloshing Damper," Proc. 42nd JSCE Annul Meeting, Vol.1, 1987, pp. 778-779. (In Japanese).
- Sayar, B., and Baumgarten J. R., "Linear and Nonlinear Analysis of Fluid Sloshing Damper," AIAA J., Vol. 20, No. 11, 1982, pp. 1534-1538.
- Shimizu, T., and Hayama, S., "Nonlinear Response of Sloshing Based on the Shallow Water Wave Theory". JSME International Journal. Vol. 30, No.263, 1987, pp. 806-813.
- Sogabe, K. and Shibata, H., "Response Analysis on Sloshing of Liquid in a Cylindrical Storage." Report of IIS, Univ. of Tokyo, Vol.26, No.3, 1974, pp.119-121. (In Japanese).
- Stoker, J.J., "Nonlinear Vibration," Wiley, Newyork, 1950.
- Sun, L. M., Fujino, Y., Pacheco, B. M., and Chaiseri, P., "Modelling of Tuned Liquid Damper (TLD)," Proc. 8th Int. Conf. on Wind Eng., London, Canada, 1991, 12pp.
- Sun, L. M., Fujino, Y., Pacheco, B. M., and Isobe, M., "Nonlinear Waves and Dynamic Pressures in Rectangular TLD - Simulation and Experimental Verification -," J. Struc. Eng./Earthq. Eng., Proc. SCE., Vol. 6, No. 2, 1989, pp.251-262.
- Tanahashi, T., "Development of FEM Algorithm for the High Reynolds Flow Problem," Research Report 63613514, Faculty of Science, Univ. of Keio, 1989. (In Japanese).
- Ueda, T., Nakagaki, R., and Arima, K., "Suppression Effect by TSD in Tower of Cable- Stayed Bridge," Proc. 11th Wind Eng. Symposium in Japan, 1990, pp.97-102. (In Japanese).
- Vandorn, W. G., "Boundary Dissipation of Oscillatory Waves, J. of Fluid Mechanics, " Vol. 24, part 4, 1966, pp.769-779.
- Warburton, G. B., and Ayorinde E. O., "Optimum Absorber Parameters for Simple Systems," Int. Jour. of Earthq. Eng. and Struct. Dynamics, Vol. 8, 1980, pp. 197-217.
- Watanabe, S., "Method of Vibration Reduction, " Proc. Japan Naval Arch. Soc. Symp., 1969, pp.156-179. (In Japanese).

- Welt, F., Modi, V. J., "Vibration Damping Through Liquid Sloshing: Part I --- A Nonlinear Analysis, Part II --- Experimental Results," Proc. Diagnostics, Vehicle Dyna. and Special Topics, ASME, Design Engineering Division (DE), Vol. 18-5, 1989, pp. 149-165.
- Yamaguchi, H., Harnpornchai, N., "Fundamental Characteristics of Multiple Tuned Mass Damper," Earthquake Eng. and Structural Dynamics, 1991. (Under prepare).
- Yoneda, M., et al., "A Practical Study of Tuned Liquid Damper with Application to the Sakitama Bridge," J. of Wind Engineering, Japan Association for Wind Engineering, No.41, 1989, pp. 105-106. (In Japanese).

NOTATIONS

The following symbols are used in this paper:

- A = amplitude of base motion of TLD;
- a = half length of TLD tank;
- b = width of TLD tank;
- ΔE = energy loss in TLD per cycle;
- $\Delta E'$ = dimensionless energy loss in TLD per cycle;
- $\varepsilon = h/a$, ratio of liquid depth to half length of TLD tank;
- E_{input} = energy input into TLD;
- $\Phi = \Phi(x, z, t)$, potential function;
- F = base shear force of TLD;
- F_m = amplitude of base shear force, F ;
- F'_m = dimensionless amplitude of base shear force;
- f = excitation frequency;
- f_w, f_s = fundamental natural frequencies of liquid motion and structure respectively;
- g = gravity acceleration;
- h = depth of liquid;
- η = free surface elevation of liquid;
- η_0 = free surface elevation of liquid near the end wall of TLD tank;
- η_{max}, η_{min} = maximum and minimum of liquid free surface elevation at the end wall of TLD tank in one cycle;
- η'_{max}, η'_{min} = dimensionless maximum and minimum of liquid free surface elevation at the end wall of TLD tank in one cycle;
- h_b = depth of boundary layer near the bottom of TLD tank;
- k = wave number;
- λ = damping coefficient of liquid;
- λ_w = damping coefficient of water;
- m = ratio of liquid mass to structural mass;
- m_s = mass of structure;
- k_s = stiffness of structure;
- ξ_s = damping ratio of structure;
- m_w = mass of liquid;
- n = division number of x for numerical simulation;

- p = pressure in liquid;
- p_o = pressure on free surface of liquid;
- P_o, P_n = liquid-induced pressure forces acting on the left and right end wall of TLD tank respectively;
- ρ = density of liquid;
- ν = kinematic viscosity of liquid;
- S = free surface contamination factor of liquid;
- T = period of excitation;
- t = time;
- t_b = shear stress near the bottom of TLD tank;
- T_s = fundamental natural period of structure;
- T_w = fundamental natural period of liquid sloshing motion;
- $u(\eta)$ = horizontal velocity of liquid particle on free surface;
- u, w = horizontal and vertical velocities of liquid particle, respectively;
- ω = angle frequency of excitation;
- ω_s = angle natural frequency of structure;
- x, z = local Cartesian coordinate system; and
- x_s = base motion of TLD in a fixed Cartesian coordinate system.

RESUME

NAME: Limin SUN
BORN: November 13, 1963
Inner Mongolia, CHINA
NATIONALITY: CHINA
TITLE: Graduate student of doctoral course
ADDRESS: Department of Civil Engineering
University of Tokyo
Hongo 7-3-1, Bunkyo-ku
Tokyo 113, JAPAN
TELEPHONE: (03) 3812-2111 Ext. 6099
FAX: (03)3812-4977
E-mail: e35288@tansei.cc.u-tokyo.ac.jp
HOME ADDRESS: 17-16, Qingnian-street #8, Kun-Qiu.
Baotou, Inner Mongolia
CHINA
EDUCATION: M.E., Civil Engineering, 1988, The University of Tokyo, Tokyo, JAPAN
B.E., Civil Engineering, 1985, Tsinghua University, Beijing, CHINA
SCHOLARSHIP: Japanese Government Scholarship (US\$1,300-1,400/month)
(1986 to present)
THESES: Doctorate:
Semi-Analytical Modelling and Damping Control of Tuned Liquid Damper
(TLD).
Master's:
Simulation of Nonlinear Waves in Rectangular Tuned Liquid Damper
(TLD).
PUBLICATIONS:
SUN, L.M., FUJINO, Y., PACHECO, B. M., and ISOBE, Masahiko: (Dec, 1988) Simulation of nonlinear waves in rectangular tuned liquid damper (TLD), Proc. Symposium of Wind Engineering, Japan. p361-366. (In Japanese).
CHASERI, P., SUN, L. M., FUJINO, Y., and PACHECO, B. M.: (Jan, 1989) On wave behavior consideration in tuned liquid damper (TLD), Proc. of

EASEC-2 2nd East Asia- Pacific Conf. on Structural Engineering & Construction, Thailand.

FUJINO, Y., PACHECO, B. M., SUN, L. M., and CHAISERI, P.: (Feb, 1989) Tuned liquid damper (TLD) for suppressing horizontal motion of structures -- Investigation on nonlinear waves in TLD and TLD-structure interaction -- , Proc, of DAMPING 89, Florida.

SUN, L. M., CHAISERI, P., PACHECO, B. M., FUJINO, Y., and ISOBE, M.: (June, 1989) Tuned liquid damper (TLD) for suppressing wind-induced vibration of structures, Proc. the second ASIA-PACIFIC SYMPOSIUM ON WIND ENGINEERING, Beijing.

FUJINO, Y., PACHECO, B. M., SUN, L. M., CHAISERI, P., and ISOBE, M.: (Mar, 1989) Simulation of nonlinear waves in rectangular tuned liquid damper (TLD) and its verification. J. of Structural Engineering (JSCE), Vol. 35A, p561-574. (IN Japanese).

SUN, L. M., PACHECO, B. M., FUJINO, Y., and CHAISERI, P.: (Oct, 1989) Effect of liquid viscosity on TLD performance -- Experiment and Simulation -- , Proc. of Annual meeting of JSCE, p732-733.

CHAISERI, P., PACHECO, B. M., FUJINO, Y., SUN, L. M., and FUJII, K.: (Oct, 1989) Forced excitation study on the effect of container shape on tuned liquid damper, Proc. of Annual meeting of JSCE, p734-735

SUN, L. M., FUJINO, Y., PACHECO, B. M., and ISOBE, M.: (Oct, 1989) Nonlinear waves and dynamic pressures in rectangular tuned liquid damper (TLD) -- simulation and experimental verification -- , Structural Eng./Earthquake Eng. Vol.6. No.2, p251s- 262s.

CHAISERI, P., FUJINO, Y., PACHECO, B. M., and SUN, L. M.: (Oct, 1989) Interaction of tuned liquid damper (TLD) and structure -- theory, experimental verification and application --, Structural Eng./Earthquake Eng. Vol.6. No.2, p273s-282s.

FUJINO, Y., PACHECO, B. M., CHAISERI, P., SUN, L. M., and KOGA, K.: (Dec, 1989) Damping of liquid motion in tuned liquid damper (TLD), Proc. of Annual Meeting of Wind Engineering, Japan. (In Japanese).

FUJINO, Y., PACHECO, B.M., SUN, L. M., and CHAISERI, P.: (1990) Tuned liquid damper for suppressing horizontal motion of structures, (Submitted to ASCE).

FUJINO, Y., SUN, L.M. and KOGA, K.: (1991) Simulation and experiment on tuned liquid damper subjected to pitching motion, J. of Structural Eng., JSCE, Vol.37A, p805-814. (In Japanese).

SUN, L. M., FUJINO, Y., PACHECO, B. M., and CHAISERI, P.: (1991) Modelling of tuned liquid damper (TLD), Proc. of Eighth International Conference on Wind Engineering, London, Ontario, Canada.

APPENDIX A Derivation of Basic Equations for Liquid Sloshing Under Horizontal Motion

A. 1 Governing Equations and Boundary Conditions

As shown in Fig. A.1, the liquid motion is assumed to develop only in x-z plane and is two-dimensional. Liquid is assumed as incompressible, irrotational fluid, and the pressure at liquid free surface is constant. The following discussion is restricted to long period oscillation and continuous surface boundary condition (no breaking waves).

The full equations governing the liquid sloshing are the continuity equation and the usual two-dimensional Navier Stokes equations for an incompressible fluid, namely,

$$\frac{\partial u}{\partial x} + \frac{\partial w}{\partial z} = 0, \quad (\text{A.1})$$

$$\frac{\partial u}{\partial t} + u \frac{\partial u}{\partial x} + w \frac{\partial u}{\partial z} = -\frac{1}{\rho} \frac{\partial p}{\partial x} + \nu \left(\frac{\partial^2 u}{\partial x^2} + \frac{\partial^2 u}{\partial z^2} \right) - \ddot{x}_s, \quad (\text{A.2})$$

$$\frac{\partial w}{\partial t} + u \frac{\partial w}{\partial x} + w \frac{\partial w}{\partial z} = -\frac{1}{\rho} \frac{\partial p}{\partial z} + \nu \left(\frac{\partial^2 w}{\partial x^2} + \frac{\partial^2 w}{\partial z^2} \right) - g, \quad (\text{A.3})$$

where u, w are the velocities of liquid particle in the x-direction and z-direction, respectively. p is pressure. ρ, ν are respectively the density and kinematic viscosity of liquid.

For liquid having relatively small viscosity, the effect of internal friction in the fluid is appreciable only in the boundary layer. The flow outside the boundary layer may be considered as potential flow, and the equations of motion become

$$\frac{\partial u}{\partial t} + u \frac{\partial u}{\partial x} + w \frac{\partial u}{\partial z} = -\frac{1}{\rho} \frac{\partial p}{\partial x} - \ddot{x}_s \quad (-(h-h_b) \leq z \leq \eta), \quad (\text{A.4})$$

$$\frac{\partial w}{\partial t} + u \frac{\partial w}{\partial x} + w \frac{\partial w}{\partial z} = -\frac{1}{\rho} \frac{\partial p}{\partial z} - g \quad (-(h-h_b) \leq z \leq \eta), \quad (\text{A.5})$$

where h_b is the thickness of the boundary layer.

The equations of motion inside boundary layer are

$$\frac{\partial u}{\partial t} + u \frac{\partial u}{\partial x} + w \frac{\partial u}{\partial z} = -\frac{1}{\rho} \frac{\partial p}{\partial x} + \nu \frac{\partial^2 u}{\partial z^2} - \ddot{x}_s \quad (-h \leq z \leq -(h-h_b)), \quad (A.6)$$

$$\frac{1}{\rho} \frac{\partial p}{\partial z} = -g \quad (-h \leq z \leq -(h-h_b)). \quad (A.7)$$

The boundary conditions are

$$u = 0 \quad \text{on the end wall } (x = \pm a), \quad (A.8)$$

$$w = 0 \quad \text{on the bottom } (z = -h), \quad (A.9)$$

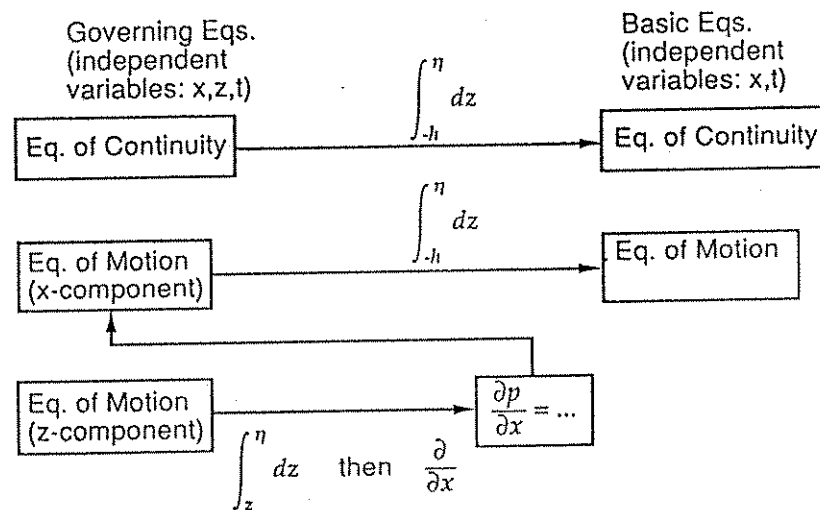
$$w = \frac{D\eta}{Dt} = \frac{\partial \eta}{\partial t} + u \frac{\partial \eta}{\partial x} \quad \text{on the free surface } (z = \eta), \quad (A.10)$$

$$p = p_0 = \text{constant} \quad \text{on the free surface } (z = \eta). \quad (A.11)$$

A. 2 Derivation of Basic Equations

Based on the shallow water wave theory, the velocity potential Φ is assumed for the main flow. The governing equations are integrated with respect to z since the liquid depth considered in this study is shallow and the horizontal velocity of liquid particle is a weak function of z . The damping of liquid sloshing due to the boundary layer and the free surface is included in the equations. The flow chart of derivation of basic equation is shown in Fig. A.2.

Figure A.2 The Flow Chart of Derivation of Basic Equation.



For the flow outside the boundary layer, a velocity potential Φ is assumed, based on the shallow water wave theory, as

$$\Phi(x, z, t) = G(x, t) \cosh(k(h+z)), \quad (\text{A.12})$$

where G is a arbitrary function. The velocities of liquid particle and their differentials can be expressed as

$$u = \frac{\partial \Phi}{\partial x} = \frac{\partial G}{\partial x} \cosh(k(h+z)), \quad (\text{A.13})$$

$$w = \frac{\partial \Phi}{\partial z} = kG \sinh(k(h+z)), \quad (\text{A.14})$$

$$w = -\frac{1}{k} \frac{\partial u}{\partial x} G \tanh(k(h+z)), \quad (\text{A.15})$$

$$\frac{\partial w}{\partial t} = -\frac{1}{k} \frac{\partial^2 u}{\partial x \partial t} G \tanh(k(h+z)), \quad (\text{A.16})$$

$$\frac{\partial w}{\partial x} = \frac{\partial u}{\partial z} = k u \tanh(k(h+z)). \quad (\text{A.17})$$

At the free surface,

$$w(\eta) = -\frac{1}{k} \frac{\partial u(\eta)}{\partial x} T_H, \quad (\text{A.18})$$

$$\frac{\partial w(\eta)}{\partial x} = -\frac{1}{k} \frac{\partial^2 u(\eta)}{\partial x \partial t} T_H, \quad (\text{A.19})$$

$$\frac{\partial w(\eta)}{\partial x} = \frac{\partial u(\eta)}{\partial z} = k(\eta) T_H, \quad (\text{A.20})$$

where $T_H = \tanh(k(h+\eta))$.

Neglecting the thickness of boundary layer and integrating the continuity equation (A.1) with respect to z , the continuity equation can be approximately expressed, with the aid of Eqs. (A.9) and (A.10), as

$$\frac{\partial \eta}{\partial t} + h\sigma \frac{\partial(\phi u(\eta))}{\partial x} = 0, \quad (\text{A.21})$$

where

$$\sigma = \frac{\tanh(kh)}{kh}, \quad (A.22)$$

$$\phi = \frac{\tanh(k(h+\eta))}{\tanh(kh)}. \quad (A.23)$$

The equation of motion in integral form is derived as following. First, to get the expression for $(1/\rho) (\partial p/\partial x)$, Eq. (A.3) is integrated with respect to z and then differentiated with respect to x . With the help of Eqs. (A.13) to (A.20), as a result, the $(1/\rho) (\partial p/\partial x)$ is expressed as,

$$\frac{1}{\rho} \frac{\partial p}{\partial x} = g \frac{\partial \eta}{\partial x} + \left(\frac{\partial w}{\partial t} \right)_{z=\eta} \frac{\partial \eta}{\partial x} + \left(\frac{\partial u}{\partial t} \right)_{z=\eta} - \frac{\partial u}{\partial t} + \frac{1}{2} \left(\frac{\partial(u^2+w^2)}{\partial x} \right)_{z=\eta} - \frac{1}{2} \left(\frac{\partial(u^2+w^2)}{\partial x} \right). \quad (A.24)$$

Then substituting Eq. (A.24) into Eq. (A.4) and Eq. (A.6), we have

$$\begin{aligned} & \left(\frac{\partial u}{\partial t} \right)_{z=\eta} + \left(u \frac{\partial u}{\partial x} + w \frac{\partial u}{\partial z} \right)_{z=\eta} + \left(g + \left(\frac{\partial w}{\partial t} \right)_{z=\eta} \right) \frac{\partial \eta}{\partial x} \\ & = \begin{cases} -\ddot{x}_s & -(h-h_b) \leq z \leq \eta, \\ v \frac{\partial^2 u}{\partial z^2} - \ddot{x}_s & (-h \leq z \leq -(h-h_b)), \end{cases} \end{aligned} \quad (A.25)$$

Integrating Eq. (A.25) with respect to z from bottom to free surface:

$$\left(\frac{\partial u}{\partial t} \right)_{z=\eta} + g \frac{\partial \eta}{\partial x} + \left(u \frac{\partial u}{\partial x} + w \frac{\partial u}{\partial z} \right)_{z=\eta} + \left(\frac{\partial w}{\partial t} \right)_{z=\eta} \frac{\partial \eta}{\partial x} = \frac{v}{(\eta+h)} \int_{-h}^{-(h-h_b)} \frac{\partial^2 u}{\partial z^2} dz - \ddot{x}_s. \quad (A.26)$$

This equation, which is independent of z , is the integral form of the equations of motion. Each terms in Eq. (A.26) can be expressed in terms of the horizontal velocity at the free surface $u(\eta)$, the surface elevation η and their differentials as following.

$$\left(u \frac{\partial u}{\partial x} + w \frac{\partial u}{\partial z} \right)_{z=\eta} = (1-T_H^2) \left(u \frac{\partial u}{\partial x} \right)_{z=\eta}, \quad (A.27)$$

$$\left(\frac{\partial w}{\partial t} \right)_{z=\eta} \frac{\partial \eta}{\partial x} = gh\sigma\phi \frac{\partial^2 \eta}{\partial x^2} \frac{\partial \eta}{\partial x}, \quad (A.28)$$

$$\frac{\nu}{(\eta+h)} \int_{-h}^{-(h-h_b)} \frac{\partial^2 u}{\partial z^2} dz = -\lambda u(\eta), \quad (\text{A.29})$$

where λ is called the damping coefficient and will be explained in Section A.3. Thus Eq. (A.26) can be equivalently written in the form,

$$\frac{\partial u(\eta)}{\partial t} + (1-T_H^2) u(\eta) \frac{\partial u(\eta)}{\partial x} + g \frac{\partial \eta}{\partial x} + gh\sigma\phi \frac{\partial^2 \eta}{\partial x^2} \frac{\partial \eta}{\partial x} = -\lambda u(\eta) - \ddot{x}_s. \quad (\text{A.30})$$

The basic equations are Eqs.(A.21) and (A.30).

A.3 Damping of Liquid Sloshing

The dissipation term (Eq. (A.29)) is due to the boundary layer, and can be simplified in following procedure.

$$\nu \int_{-h}^{-(h-h_b)} \frac{\partial^2 u}{\partial z^2} dz = \frac{1}{\rho} (\tau_{z=-(h-h_b)} - \tau_{z=-h}), \quad (\text{A.31})$$

where

$$\tau_b \equiv \rho \nu \frac{\partial u}{\partial z},$$

is shear stress. It is assumed that the shear stress outside the boundary layer is very small and can be neglected. Thus,

$$\nu \int_{-h}^{-(h-h_b)} \frac{\partial^2 u}{\partial z^2} dz = \frac{1}{\rho} \tau_b, \quad (\text{A.32})$$

where $\tau_b \equiv \tau_{z=-h}$, is the shear stress at the bottom.

From the linear and laminar boundary layer theory [Lamb 1932] and considering sinusoidal excitation, τ_b is $\pi/4$ out of phase with the horizontal velocity component of liquid just outside the boundary layer, u_b . Using the concept of equivalence of energy loss per cycle, the τ_b can be expressed as

$$\tau_b = \rho \frac{1}{\sqrt{2}} \sqrt{\omega \nu} u_b, \quad (\text{A.33})$$

in which $1/\sqrt{2}$ is an equivalence factor due to the phase lag $\pi/4$, and ω is the angular frequency of the liquid sloshing. In the present study, since the liquid depth is shallow and the liquid sloshing is shallow wave, we assumed that $u_b = u(\eta)$. Thus,

$$\tau_b = \rho \frac{1}{\sqrt{2}} \sqrt{\omega \nu} u(\eta). \quad (\text{A.34})$$

Miles [1967] has studied the damping of surface wave in a rectangular tank and suggested that the dissipation term can be multiplied by $(1+2h/b+S)$, where b is the width of the tank, to account for the dissipation due to the side wall friction and the liquid surface contamination. $2h/b$ is an equivalent coefficient of the damping effect per width due to the side wall boundary layer. It is regarded that the friction of side wall boundary layer is the same as that of bottom boundary layer. S is a "surface contamination" factor which can vary between 0 and 2. A value of unity will be used in this study, which corresponds to the establishment of "the fully contaminated surface".

The dissipation term with the effects of side walls and the free surface is

$$\frac{\nu}{(\eta+h)} \int_{-h}^{-(h-hb)} \frac{\partial^2 u}{\partial z^2} dz = - \frac{1}{\eta+h} \frac{1}{\sqrt{2}} \sqrt{\omega \nu} \left(1 + \frac{2h}{b} + S\right) u(\eta) = -\lambda u(\eta), \quad (\text{A.35})$$

where

$$\lambda = \frac{1}{\eta+h} \frac{1}{\sqrt{2}} \sqrt{\omega \nu} \left(1 + \frac{2h}{b} + S\right). \quad (\text{A.36})$$

APPENDIX B Solution of Basic Equations for Liquid Sloshing Under Horizontal Motion

B. 1 Nondimensionalization of Basic equation

The variables are nondimensionalized as follows:

$$\begin{aligned} x' &= \frac{x}{a}, & z' &= \frac{z}{h}, & \eta' &= \frac{\eta}{h}, & \varepsilon &= \frac{h}{a}, \\ u' &= \frac{u}{C_0}, & t' &= \frac{t}{t_0}, & k' &= ka, \\ \ddot{x}' &= \frac{t_0^2}{a} \ddot{x}_s, & \omega' &= \omega t_0, \end{aligned} \quad (B.1)$$

where $C_0 = \sqrt{gh}$ is wave velocity and $t_0 = a/C_0$. The variables with a prime are dimensionless ones.

Substituting Eq. (B.1) into Eqs. (A.21), (A.30) and (A.8), we obtain the dimensionless basic equations,

$$\frac{\partial \eta'}{\partial t'} + \sigma \frac{\partial \phi(u'(\eta))}{\partial x'} = 0, \quad (B.2)$$

$$\frac{\partial u'(\eta)}{\partial t'} + (1 - T_H^2) u'(\eta) \frac{\partial u'(\eta)}{\partial x'} + \frac{\partial \eta'}{\partial x'} + \sigma \phi \varepsilon^2 \frac{\partial^2 \eta'}{\partial x'^2} \frac{\partial \eta'}{\partial x'} = -\lambda' u'(\eta) - \dot{x}'_s, \quad (B.3)$$

and the boundary condition

$$u'(\eta) = 0 \quad \text{on the end wall } (x' = \pm 1). \quad (B.4)$$

The dimensionless damping coefficient λ' is

$$\lambda' = \frac{1}{\eta' + 1} \frac{1}{\sqrt{2\varepsilon C_0}} \sqrt{\omega v} (1 + \frac{2h}{b} + S). \quad (B.5)$$

B. 2 Discretization of Basic Equation

The basic equations are simultaneous differential equations. First, the equations are discretized with respect to x into n divisions. Then the simultaneous difference equations are obtained and are solved using Runge-Kutta-Gill method. It should be noted that the dispersion relation of the basic

equations is replaced by that produced due to the discretization of x in this procedure. The latter is dependent on the number of division n .

Considering first mode of liquid sloshing, to which corresponding dimensionless wave number,

$$k' = \frac{\pi}{2}. \quad (B.6)$$

Writing the basic equations (B.2) and (B.3) in the form,

$$\frac{\partial \eta'}{\partial t'} + \sigma \frac{\partial \phi(u'(\eta))}{\partial x'} = 0, \quad (B.7)$$

$$\frac{\partial u'(\eta)}{\partial t'} + \frac{\partial \eta'}{\partial x'} + H \frac{\partial K}{\partial x'} + C \frac{\partial I}{\partial x'} = -\lambda' u'(\eta) - \dot{x}'_s, \quad (B.8)$$

where

$$H = \frac{1}{2} (1 - T_R^2), \quad (B.9)$$

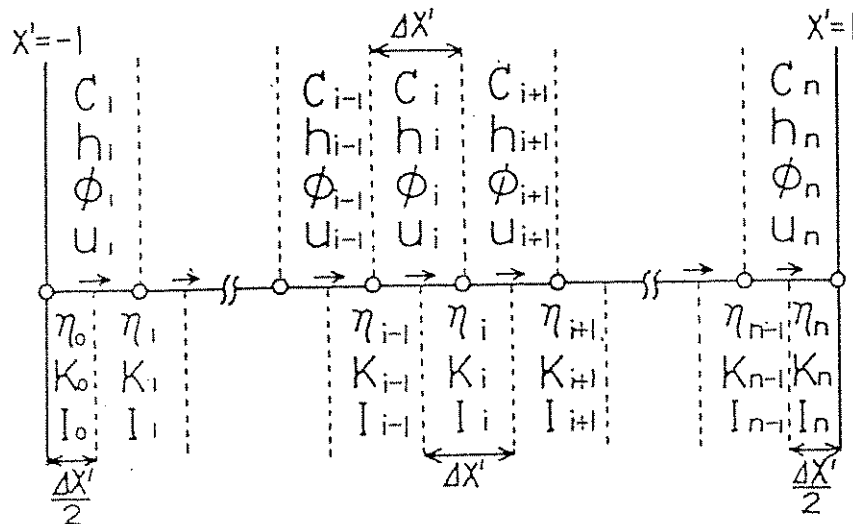
$$K = u'^2, \quad (B.10)$$

$$C = \sigma \phi \epsilon^2, \quad (B.11)$$

$$I = \frac{1}{2} \frac{\partial \eta'^2}{\partial x'}. \quad (B.12)$$

Discretizing the container length as shown in Fig. B.1, the difference basic equation are obtained.

Figure B.1 The Discretization with respect to x .



$$\frac{d\eta'_i}{dt'} = \frac{\sigma}{\Delta x'} (\phi_i u'(\eta)_{i-1} - \phi_{i-1} u''(\eta)_{i-1}) \quad (i=1 \sim n-1), \quad (B.13)$$

$$\frac{d\eta'_0}{dt'} = -\frac{2\sigma}{\Delta x'} \phi_1 u'(\eta)_1, \quad (B.14)$$

$$\frac{d\eta'_n}{dt'} = \frac{2\sigma}{\Delta x'} \phi_n u'(\eta)_n, \quad (B.15)$$

$$\frac{du'_n}{dt'} = \frac{1}{\Delta x'} (\eta'_{i-1} - \eta'_i + H_i(K_{i-1} - K_i) + C_i(I_{i-1} - I_i)) - \lambda'_i u'_i - \sigma \ddot{x}_s \quad (i=1 \sim n), \quad (B.16)$$

where,

$$\Delta x' = \frac{2}{n}, \quad (B.17)$$

$$\phi_i = \tanh(k' \epsilon (1 + (\eta'_{i-1} + \eta'_i)/2)) / \tanh(k' \epsilon) \quad (i=1 \sim n), \quad (B.18)$$

$$H_i = (1 - (\phi_i \tanh(k' \epsilon))^2) \quad (i=1 \sim n), \quad (B.19)$$

$$K_i = ((u'_i + u'_{i+1})/2)^2 \quad (i=1 \sim n-1), \quad (B.20)$$

$$I_i = (((\eta'_{i+1} + \eta'_{i-1})/(2\Delta x'))^2)/2 \quad (i=1 \sim n-1), \quad (B.21)$$

and

$$\lambda'_i = \frac{1}{1 + (\eta'_{i+1} + \eta'_i)/2} \frac{\sqrt{\omega v}}{\sqrt{2} \epsilon C_0} (1 + 2h/b + S). \quad (B.22)$$

Form the boundary conditions,

$$K_0 = K_n = 0, \quad (B.23)$$

$$I_0 = I_n = 0. \quad (B.24)$$

To replace the dispersion relation of the basic equations by that due to the discretization, the division number is determined by,

$$n = \pi / (2 \arccos \sqrt{\tanh(\pi \epsilon \epsilon) / (2 \tanh(\pi \epsilon / 2))}). \quad (B.25)$$

After determining the division number n , the difference basic equations are solved numerically by using Runge-Kutta-Gill method and $u(\eta)$ and η can be obtained.

B.3 Runge-Kutta-Gill Method

The difference basic equations (B.13,14) and (B.15,16) can be expressed in the vector form,

$$\frac{d\eta}{dt'} = f(t, \eta, u), \quad (B.26)$$

$$\frac{du}{dt'} = g(t, \eta, u), \quad (B.27)$$

where

$$\eta = (\eta'_0, \eta'_1, \dots, \eta'_i, \dots, \eta'_n), \quad (B.28)$$

$$u = (u'_0, u'_1, \dots, u'_i, \dots, u'_n). \quad (B.29)$$

Initial conditions are

$$\eta_0 = 0 \quad (t=0), \quad (B.30)$$

$$u_0 = 0 \quad (t=0), \quad (B.31)$$

where the subscript denotes the time step.

The common formulas of Runge-Kutta-Gill method are

$$\eta_{m+1} = \eta_m + \frac{\Delta t}{6} (K_1 + (2-\sqrt{2})K_2 + (2+\sqrt{2})K_3 + K_4), \quad (B.32)$$

$$u_{m+1} = u_m + \frac{\Delta t}{6} (L_1 + (2-\sqrt{2})L_2 + (2+\sqrt{2})L_3 + L_4), \quad (B.33)$$

where, Δt is increment of time t and

$$K_1 = f(t_m, \eta_m, u_m), \quad (B.34)$$

$$L_1 = g(t_m, \eta_m, u_m), \quad (B.35)$$

$$K_2 = f(t_m + \frac{\Delta t}{2}, \eta_m + \frac{\Delta t}{2}K_1, u_m + \frac{\Delta t}{2}L_1), \quad (B.36)$$

$$L_2 = g(t_m + \frac{\Delta t}{2}, \eta_m + \frac{\Delta t}{2}K_1, u_m + \frac{\Delta t}{2}L_1), \quad (B.37)$$

$$K_3 = f(t_m + \frac{\Delta t}{2}, \eta_m + \frac{\sqrt{2}-1}{2}\Delta t K_1 + (1-\frac{\sqrt{2}}{2})\Delta t K_2, u_m + \frac{\sqrt{2}-1}{2}\Delta t L_1 + (1-\frac{\sqrt{2}}{2})\Delta t L_2), \quad (B.38)$$

$$L_3 = g(t_m + \frac{\Delta t}{2}, \eta_m + \frac{\sqrt{2}-1}{2}\Delta t K_1 + (1 + \frac{\sqrt{2}}{2})\Delta t K_2, u_m + \frac{\sqrt{2}-1}{2}\Delta t L_1 + (1 + \frac{\sqrt{2}}{2})\Delta t L_2), \quad (B.39)$$

$$K_4 = f(t_m + \frac{\Delta t}{2}, \eta_m - \frac{\sqrt{2}-1}{2}\Delta t K_2 + (1 + \frac{\sqrt{2}}{2})\Delta t K_3, u_m - \frac{\sqrt{2}-1}{2}\Delta t L_2 + (1 + \frac{\sqrt{2}}{2})\Delta t L_3), \quad (B.40)$$

$$L_4 = g(t_m + \frac{\Delta t}{2}, \eta_m - \frac{\sqrt{2}-1}{2}\Delta t K_2 + (1 + \frac{\sqrt{2}}{2})\Delta t K_3, u_m - \frac{\sqrt{2}-1}{2}\Delta t L_2 + (1 + \frac{\sqrt{2}}{2})\Delta t L_3). \quad (B.41)$$

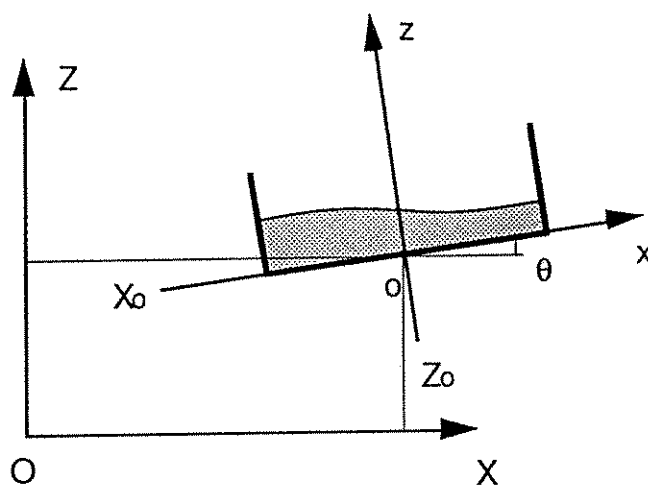
APPENDIX C Derivation and Solution of Basic Equations for Liquid Sloshing Under Pitching Motion

C.1 The derivation of basic equations

The theoretical model is based on the shallow wave theory and the nonlinearity has been taken into account. The approach employed here is similar to that used in App. A

Governing Equations

Figure C.1 The TLD tank under Pitching Motion.



The motion of TLD tank is shown in Fig. C.1. The coordination system XOZ is fixed and the another coordination system xoz moves with TLD tank. The motion of TLD tank can be expressed by X_0 , Z_0 , and θ .

Equation of Continuity:

$$\frac{\partial u}{\partial x} + \frac{\partial w}{\partial z} = 0. \quad (C.1)$$

Equations of motion (Eular's equations):

$$\frac{\partial u}{\partial t} + u \frac{\partial u}{\partial x} + w \frac{\partial u}{\partial z} = -\frac{1}{\rho} \frac{\partial p}{\partial x} + a_x \quad (h_b \leq z \leq h + \eta), \quad (C.2)$$

$$\frac{\partial w}{\partial t} + u \frac{\partial w}{\partial x} + w \frac{\partial w}{\partial z} = -\frac{1}{\rho} \frac{\partial p}{\partial z} + a_z \quad (h_b \leq z \leq h + \eta), \quad (C.3)$$

where a_x and a_z are the inertia forces.

Boundary conditions:

$$u = 0 \quad (x = \pm a) \quad (C.4)$$

$$w = 0 \quad (z = 0) \quad (C.5)$$

$$w = \frac{\partial \eta}{\partial t} + u \frac{\partial \eta}{\partial x} \quad (z = h + \eta) \quad (C.6)$$

$$p = p_o = \text{const.} \quad (z = h + \eta) \quad (C.7)$$

The liquid damping is only considered in the boundary layer near the solid walls, and the treatment is similar to that proposed in App. A. For simplicity, the equations of motion are taken the form of Euler's Equation. The damping effect will be added lately.

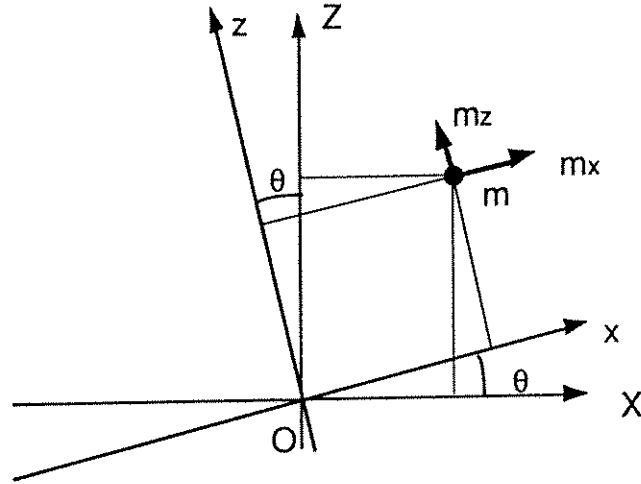
The Inertia Forces in a Rotational Coordination System

As shown in Fig. C.2. the fixed rectangular coordination is XOZ, and another rectangular coordination system xoz for which the origin is at O rotates around O with angular deformation q . The inertia forces under the system xoy are

$$m\ddot{x} = m(-g \sin \theta + 2\dot{z}\dot{\theta} + x\dot{\theta}^2 + z\ddot{\theta}) \quad (C.8)$$

$$m\ddot{z} = m(-g \cos \theta - 2\dot{x}\dot{\theta} + z\dot{\theta}^2 - x\ddot{\theta}) \quad (C.9)$$

Figure C.2 The Inertia Forces in a Rotational Coordination System.



where the 1st term is the effect of gravity; the 2nd term is Coriolis' force; the 3rd term is centrifugal force, and the 4th term is tangent acceleration force.

Comparison of the order of external forces.

$$\begin{cases} a_x = -g \sin \theta + 2\dot{\theta}w + \ddot{\theta}z + \dot{\theta}^2 x - \ddot{X}_o \cos \theta - \ddot{Z}_o \sin \theta & (C.10) \\ a_z = -g \cos \theta - 2\dot{\theta}u - \ddot{\theta}x + \dot{\theta}^2 z + \ddot{X}_o \sin \theta - \ddot{Z}_o \cos \theta & (C.11) \end{cases}$$

Assuming that:

$$\theta \sim \hat{\theta} e^{i\omega t}, \quad (C.12)$$

$$x \sim h \hat{\theta} e^{i\omega t}, \quad (C.13)$$

$$z \sim a \hat{\theta} e^{i\omega t}. \quad (C.14)$$

so,

$$\dot{\theta} \sim \omega \hat{\theta} e^{i\omega t}, \quad (C.15)$$

$$\dot{x} \sim \omega h \hat{\theta} e^{i\omega t}, \quad (C.16)$$

$$\dot{z} \sim \omega \hat{\theta} e^{i\omega t}. \quad (C.17)$$

And assuming that:

$$u \sim \hat{u} e^{i(kx - \omega t)} \quad (C.18)$$

$$w \sim \hat{w} e^{i\omega t} \quad (C.19)$$

so,

$$\partial_t u \sim \omega \hat{u}, \quad \partial_x u \sim k \hat{u} \quad (C.20)$$

$$\hat{w} \ll \hat{u} \quad (C.21)$$

From z-component of equations of motion, we know that

$$\omega \hat{u} \sim g \quad (C.22)$$

and for shallow liquid sloshing, $h \ll a$.

The orders of each terms in a_x and a_z are shown as follows:

$$\begin{array}{cccccc}
 a_x = -g \sin \theta + 2\dot{\theta}w + \ddot{\theta}z + \dot{\theta}^2 x - \ddot{X}_0 \cos \theta - \ddot{Z}_0 \sin \theta & & & & & \\
 \downarrow & \downarrow & \downarrow & \downarrow & \downarrow & \downarrow \\
 g\hat{\theta} & \omega\hat{\theta}\hat{w} & h\omega^2\hat{\theta} & a(\omega\hat{\theta})^2 & \ddot{X}_0 & \ddot{Z}_0\hat{\theta} \\
 \downarrow & \downarrow & \downarrow & \downarrow & \downarrow & \downarrow \times 1/(g\hat{\theta}) \\
 1 & \frac{\hat{w}}{\hat{u}} & \frac{h\omega}{\hat{u}} & \frac{a\omega\hat{\theta}}{\hat{u}} & \frac{\ddot{X}_0}{g\hat{\theta}} & \frac{\ddot{Z}_0}{g} \\
 & \ll O(1) & & \ll O(1) & &
 \end{array} \quad (C.23)$$

$$\begin{array}{cccccc}
 a_z = -g \cos \theta + 2\dot{\theta}u + \ddot{\theta}x + \dot{\theta}^2 z + \ddot{X}_0 \sin \theta - \ddot{Z}_0 \cos \theta & & & & & \\
 \downarrow & \downarrow & \downarrow & \downarrow & \downarrow & \downarrow \\
 g & w\hat{\theta}\hat{u} & aw^2\hat{\theta} & h(w\hat{\theta})^2 & \ddot{X}_0\hat{\theta} & \ddot{Z}_0 \\
 \downarrow & \downarrow & \downarrow & \downarrow & \downarrow & \downarrow \times 1/g \\
 1 & \hat{\theta} & \frac{hw}{\hat{u}} & \frac{aw\hat{\theta}}{\hat{u}} & \frac{\ddot{X}_0\hat{\theta}}{g} & \frac{\ddot{Z}_0}{g} \\
 & \ll O(1) & & \ll O(1) & &
 \end{array} \quad (C.24)$$

Neglect the term whose order $\ll O(1)$ and we get

$$\begin{cases} a_x \approx - (g + \ddot{Z}_0) \sin\theta + \ddot{\theta}z - \ddot{X}_0 \cos\theta \\ a_z \approx - (g + \ddot{Z}_0) \cos\theta - \ddot{\theta}x + \ddot{X}_0 \sin\theta \end{cases} \quad \begin{matrix} (C.25) \\ (C.26) \end{matrix}$$

Derivations

Assuming the potential function:

$$\Phi = F(x,t) \cosh(kz) \quad (C.27)$$

Integrate the equation of continuity respect to z ,

$$\frac{\partial \eta}{\partial t} + h\sigma \frac{\partial \phi u(\eta)}{\partial x} = 0 \quad (C.28)$$

where

$$\sigma = \frac{\tanh(kh)}{kh} \quad (C.29)$$

$$\phi = \frac{\tanh(k(h + \eta))}{\tanh(kh)} \quad (C.30)$$

Eliminate p in z -component of equation of motion by using x -component, and integrate the equation obtained respect to z ,

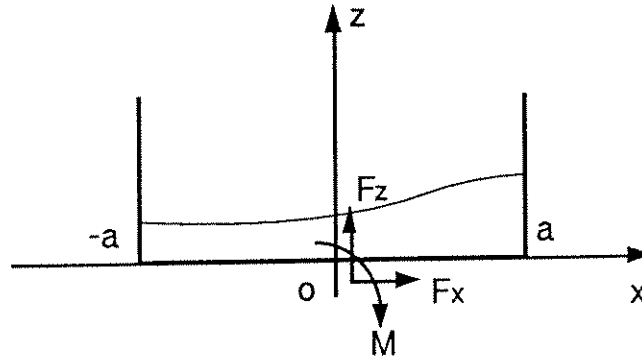
$$\begin{aligned} & \frac{\partial u(\eta)}{\partial t} + \frac{1}{2} \frac{\partial u(\eta)^2}{\partial x} + ((g + \ddot{Z}_0) \cos\theta - \ddot{X}_0 \sin\theta + \ddot{\theta}x \\ & + (g + \ddot{Z}_0) \cos\theta h\sigma\phi \frac{\partial^2 \eta}{\partial x^2}) \frac{\partial \eta}{\partial x} = - (g + \ddot{Z}_0) \sin\theta - \ddot{X}_0 \cos\theta - \lambda u(\eta) \end{aligned} \quad (C.31)$$

Forces and Moment due to Liquid Sloshing

From z -component of equation of motion, neglect the effect of vertical acceleration of liquid particles and other higher orders and consider static pressures only,

$$p - p_0 = -\rho a_z (h + \eta - z) \quad (C.32)$$

Figure C.3 The Forces and Moment due to Liquid Sloshing.



The forces and moments (Fig. C.3) due to liquid sloshing are

$$F_x = -\frac{1}{2} \rho b a_z ((h+\eta_a)^2 - (h+\eta_{-a})^2), \quad (C.33)$$

$$F_z = \int_{-a}^a \rho b a_z (h+\eta) dx, \quad (C.34)$$

$$M = -\frac{1}{6} \rho b a_z ((h+\eta_a)^3 - (h+\eta_{-a})^3) - \int_{-a}^a \rho b a_z (h+\eta) x dx. \quad (C.35)$$

Nondimensionalization

$$\begin{aligned} C_0 &\equiv \sqrt{gh}, \quad t_0 \equiv \frac{a}{C_0} \\ x' &= \frac{x}{a}, \quad z' = \frac{z}{h}, \quad \eta' = \frac{\eta}{h} \\ u' &= \frac{u}{C_0}, \quad t' = \frac{t}{t_0}, \quad k' = ka \\ \omega' &= \omega t_0, \quad \varepsilon = \frac{h}{a} \end{aligned} \quad (C.36)$$

$$\frac{\partial \eta'}{\partial t'} + \sigma \frac{\partial \phi u'(\eta)}{\partial x'} = 0 \quad (C.37)$$

$$\begin{aligned}
& \frac{\partial u'(\eta)}{\partial t'} + \frac{1}{2} \frac{\partial u'(\eta)^2}{\partial x'} \\
& + \left(\left(1 + \frac{\ddot{Z}_0}{g} \right) \cos \theta - \frac{\ddot{X}_0}{g} \sin \theta + \frac{a \ddot{\theta}}{g} x' + \left(1 + \frac{\ddot{Z}_0}{g} \right) \cos \theta h \sigma \phi \varepsilon^2 \frac{\partial^2 \eta \eta}{\partial x'^2} \right) \frac{\partial \eta \eta}{\partial x'} \quad (C.38) \\
& = - \left(1 + \frac{\ddot{Z}_0}{g} \right) \sin \theta \frac{1}{\varepsilon} - \frac{\ddot{X}_0}{g \varepsilon} \cos \theta - \lambda u'(\eta)
\end{aligned}$$

B.C's:

$$u' = 0 \quad (x' = \pm 1). \quad (C.39)$$

In this study, the period of sloshing is regarded long and the deformation is small, the dimensionless basic equations are

$$\frac{\partial \eta'}{\partial t'} + \sigma \frac{\partial \phi u'(\eta)}{\partial x'} = 0 \quad (C.40)$$

$$\begin{aligned}
& \frac{\partial u'(\eta)}{\partial t'} + \frac{1}{2} \frac{\partial u'(\eta)^2}{\partial x'} \\
& + (\cos \theta + \cos \theta h \sigma \phi \varepsilon^2 \frac{\partial^2 \eta \eta}{\partial x'^2}) \frac{\partial \eta \eta}{\partial x'} \quad (C.41) \\
& = - \frac{1}{\varepsilon} \sin \theta - \frac{\ddot{X}_0}{g \varepsilon} \cos \theta - \lambda u'(\eta)
\end{aligned}$$

Discretization

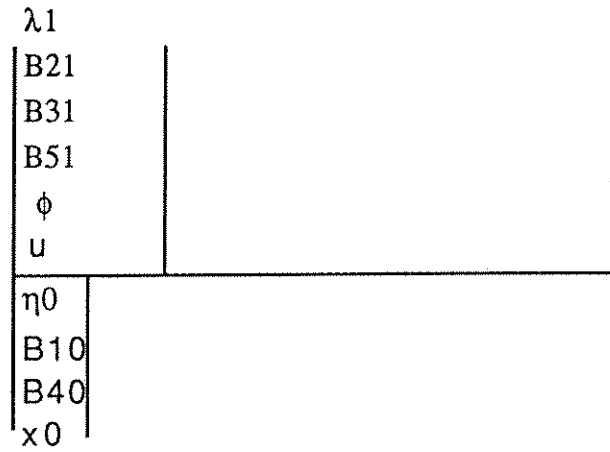
The basic equations can be rewritten in the form of:

$$\frac{\partial u(\eta)}{\partial t} + \frac{\partial B_1}{\partial x} + B_2 \frac{\partial \eta}{\partial x} + B_3 \frac{\partial B_4}{\partial x} = B_5 - \lambda u(\eta) \quad (C.42)$$

where

$$\begin{aligned}
B_1 &= \frac{1}{2} u(\eta)^2 \\
B_2 &= \left(1 + \frac{\ddot{Z}_0}{g} \right) \cos \theta + \frac{\ddot{X}_0}{g} \sin \theta + x' \frac{a \ddot{\theta}}{g} \\
B_3 &= \left(1 + \frac{\ddot{Z}_0}{g} \right) \sigma \phi \varepsilon^2 \cos \theta \\
B_4 &= \frac{1}{2} \left(\frac{\partial \eta}{\partial x} \right)^2 \\
B_5 &= - \left(1 + \frac{\ddot{Z}_0}{g} \right) \frac{1}{\varepsilon} \sin \theta - \frac{\ddot{X}_0}{g \varepsilon} \cos \theta
\end{aligned} \quad (C.43)$$

Figure C.4 Discretization.



The discretized equations are:

$$\left\{ \begin{array}{l} \frac{\partial \eta_i}{\partial t} = \frac{\sigma}{\Delta x} (\phi_i u_i - \phi_{i-1} u_{i-1}) \quad (i = 1 \sim n-1) \\ \frac{\partial \eta_0}{\partial t} = -\frac{2\sigma}{\Delta x} \phi_1 u_1 \\ \frac{\partial \eta_n}{\partial t} = \frac{2\sigma}{\Delta x} \phi_n u_n \end{array} \right. \quad (C.44)$$

$$\begin{aligned} \frac{\partial u_i}{\partial t} = & \frac{1}{\Delta x} (B_{1i-1} - B_{1i} + B_{2i} (\eta_{i-1} - \eta_i) \\ & + B_{3i} (B_{4i-1} - B_{4i})) + B_{5i} - \lambda' u_i \quad (i = 1 \sim n) \end{aligned} \quad (C.45)$$

Dispersion Relation:

$$n = \frac{\pi}{2 \arccos \sqrt{\frac{\tanh(\pi \epsilon)}{2 \tanh(\pi \epsilon/2)}}} \quad (C.46)$$

The basic equations are solved by using Runge-Kutta-Gill method (App. B).